



Continuous measurements of nitrous oxide isotopomers during incubation experiments

Malte Winther¹, David Balslev-Harder^{1,2}, Søren Christensen³, Anders Priemé^{4,5}, Bo Elberling⁵, Eric Crosson⁶, and Thomas Blunier¹

¹Centre for Ice and Climate, Niels Bohr Institute, University of Copenhagen, Copenhagen, Denmark

²DFM – Danish National Metrology Institute, Kgs. Lyngby, Denmark

³Section for Terrestrial Ecology, Department of Biology, University of Copenhagen, Copenhagen, Denmark

⁴Section for Microbiology, Department of Biology, University of Copenhagen, Copenhagen, Denmark

⁵Center for Permafrost, Department of Geosciences and Natural Resource Management, University of Copenhagen, Copenhagen, Denmark

⁶Picarro Inc, Santa Clara, CA 95054, USA

Correspondence: Malte Winther (malte.winther@nbi.ku.dk)

Received: 2 May 2017 – Discussion started: 16 May 2017

Revised: 26 August 2017 – Accepted: 11 September 2017 – Published: 8 February 2018

Abstract. Nitrous oxide (N₂O) is an important and strong greenhouse gas in the atmosphere. It is produced by microbes during nitrification and denitrification in terrestrial and aquatic ecosystems. The main sinks for N₂O are turnover by denitrification and photolysis and photo-oxidation in the stratosphere. In the linear N=N=O molecule ¹⁵N substitution is possible in two distinct positions: central and terminal. The respective molecules, ¹⁴N¹⁵N¹⁶O and ¹⁵N¹⁴N¹⁶O, are called isotopomers. It has been demonstrated that N₂O produced by nitrifying or denitrifying microbes exhibits a different relative abundance of the isotopomers. Therefore, measurements of the site preference (difference in the abundance of the two isotopomers) in N₂O can be used to determine the source of N₂O, i.e., nitrification or denitrification. Recent instrument development allows for continuous position-dependent $\delta^{15}\text{N}$ measurements at N₂O concentrations relevant for studies of atmospheric chemistry. We present results from continuous incubation experiments with denitrifying bacteria, *Pseudomonas fluorescens* (producing and reducing N₂O) and *Pseudomonas chlororaphis* (only producing N₂O). The continuous measurements of N₂O isotopomers reveals the transient isotope exchange among KNO₃, N₂O, and N₂. We find bulk isotopic fractionation of $-5.01\text{‰} \pm 1.20$ for *P. chlororaphis*, in line with previous results for production from denitrification. For *P. fluorescens*, the bulk isotopic frac-

tionation during production of N₂O is $-52.21\text{‰} \pm 9.28$ and $8.77\text{‰} \pm 4.49$ during N₂O reduction.

The site preference (SP) isotopic fractionation for *P. chlororaphis* is $-3.42\text{‰} \pm 1.69$. For *P. fluorescens*, the calculations result in SP isotopic fractionation values of $5.73\text{‰} \pm 5.26$ during production of N₂O and $2.41\text{‰} \pm 3.04$ during reduction of N₂O. In summary, we implemented continuous measurements of N₂O isotopomers during incubation of denitrifying bacteria and believe that similar experiments will lead to a better understanding of denitrifying bacteria and N₂O turnover in soils and sediments and ultimately hands-on knowledge on the biotic mechanisms behind greenhouse gas exchange of the globe.

1 Introduction

The atmospheric concentration of nitrous oxide (N₂O) has increased from approximately 271 ppb before industrialization to 324 ppb in 2011 (Ciais et al., 2013). This increase has resulted in (1) N₂O being the third-most important greenhouse gas, that is, N₂O has the third-highest contribution to the radiative forcing of the naturally occurring greenhouse gases (Hartmann et al., 2013), and (2) an increased production of nitrogen oxides (NO_x) in the stratosphere and thereby

increased ozone depletion (Forster et al., 2007; Kim and Craig, 1993).

Ice core records show that N₂O concentrations positively correlate with Northern Hemisphere temperature variations, e.g., during the last glacial–interglacial termination as well as over the rapid climate variations occurring during the glacial period, known as Dansgaard–Oeschger events (D–O events) (Schilt et al., 2010). However, occasionally (e.g., D–O event 15 and 17) the N₂O concentration increases long before the onset of the dramatic temperature change (Schilt et al., 2010), providing a potential early warning for rapid climate change. Isotopomers of N₂O provide information on the sources (Pérez et al., 2000, 2001; Park et al., 2011), i.e., whether N₂O originates predominately from nitrification or denitrification processes. As the conditions/circumstances leading to emissions from the two processes differ both for the marine and terrestrial sources, measuring isotopomers potentially improves our understanding of the climate conditions leading to the release of N₂O over rapid climatic changes.

The N₂O molecule has an asymmetric linear structure (N=N=O) where the position of the ¹⁵N can be determined. The positions in the N₂O molecule have been named N^α and N^β or short α and β (Yoshida and Toyoda, 2000). N₂O molecules with ¹⁵N substitution in the central and terminal positions are named ¹⁵N^α for ¹⁴N¹⁵N¹⁶O and ¹⁵N^β for ¹⁵N¹⁴N¹⁶O, respectively. The two isotopomers can be distinguished using isotope ratio mass spectrometry if measurements of the NO fragment are included. Distinction is further possible using mid-infrared spectroscopy because the rotational and vibrational conditions are different for the two isotopomers providing spectral regions where absorptions of the two isotopomers do not overlap (Waechter et al., 2008; Mohn et al., 2010, 2012; Köster et al., 2013b; Heil et al., 2014). For isotopomer measurements at low N₂O concentration (low ppm range), a joint instrument development was executed, applying cavity ring-down spectroscopy (CRDS) to enable continuous and selective measurements of the isotopomer abundances.

The isotopic composition of a sample is reported as δ values which represent the deviation of the elemental isotope ratio R_{sample} in the sample from a standard R_{std} (Eq. 1). These δ values can be calculated for bulk N₂O as well as for δ¹⁵N^α and δ¹⁵N^β. All results are reported relative to the isotopic composition of atmospheric nitrogen.

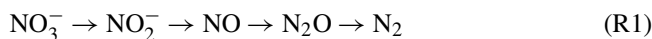
$$\delta^{15}\text{N} = \frac{R_{\text{Sample}}}{R_{\text{Std}}} - 1 \quad \text{where} \quad R = \frac{[^{15}\text{N}]}{[^{14}\text{N}]} \quad (1)$$

The N₂O bulk isotopic composition calculates as the average of δ¹⁵N^α and δ¹⁵N^β (Eq. 2) while the SP is by definition their difference (Eq. 2) (Brenninkmeijer and Röckmann, 1999; Toyoda et al., 2002).

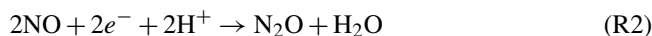
$$\text{SP} = \delta^{15}\text{N}^{\alpha} - \delta^{15}\text{N}^{\beta}, \quad \delta^{15}\text{N}^{\text{bulk}} = \frac{\delta^{15}\text{N}^{\alpha} + \delta^{15}\text{N}^{\beta}}{2} \quad (2)$$

There are multiple natural and anthropogenic sources of N₂O. The primary anthropogenic increase in N₂O emissions originate from organic and inorganic N fertilizers used for agriculture. The natural sources are primarily nitrification and denitrification in terrestrial and aquatic ecosystems (Mosier et al., 1998; Olivier et al., 1998).

Denitrification is a stepwise biological reduction process in which denitrifying bacteria ultimately produce nitrogen (N₂). Under anaerobic conditions the denitrifying bacteria use nitrate (NO₃⁻) instead of oxygen as an electron acceptor in the respiration of organic matter. Through multiple anaerobic reactions N₂ is produced as the end product of the complete denitrifying process (Reaction R1) (Firestone and Davidson, 1989).



Each of these anaerobic reactions is carried out by a genuine enzyme; i.e., the production of N₂O is caused by the reaction between nitric oxide (NO) and the enzyme nitric oxide reductase (NOR). The NOR enzyme works as a catalyst in the reduction of NO as shown in Reaction (R2) (Wrage et al., 2001; Tosha and Shiro, 2013).



The cleavage of the covalent N=O bond of N₂O leading to N₂ and H₂O is the result of N₂O reduction during bacterial denitrification (Reaction R3). According to kinetic isotope theory, the cleavage of N₂O is expected to fractionate in favor of the ¹⁵N^α molecule, due to a stronger ¹⁵N–O bond compared to the ¹⁴N–O (Popp et al., 2002), diffusion into the cell (Tilsner et al., 2003), and enzymatic reduction (Wrage et al., 2004). N₂O reduction during bacterial denitrification is therefore expected to lead to an increase in SP.



Reactions with different enzymes typically result in specific isotopic fractionation. The isotopic composition of the intermediately produced N₂O during denitrification is a consequence of multiple reaction steps. Two species of denitrifying bacteria with slightly different enzymes potentially lead to different fractionation. In this study, we compared the fractionation of two contrasting denitrifying bacteria: *Pseudomonas fluorescens* producing and reducing N₂O, and *Pseudomonas chlororaphis* producing but not reducing N₂O. Isotope effects during denitrification are diverse and species dependent (e.g., Denk et al., 2017). Our study demonstrates a new way to determine fractionation factors from continuous measurements of N₂O.

2 Method

Our objective was to perform continuous position-dependent δ¹⁵N measurements of two different bacterial cultures during

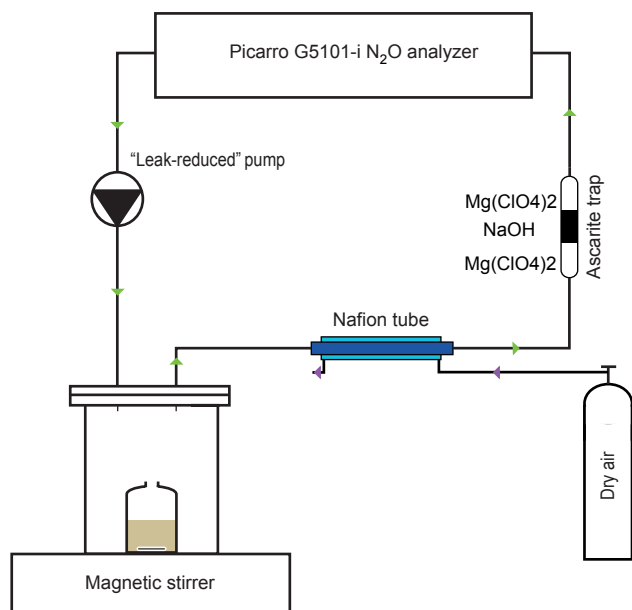


Figure 1. Simplified schematic of the incubation setup. The green and the purple arrows show the flow direction of the measuring gas and the purge gas, respectively.

incubation experiments. Using two denitrifying bacterial cultures we determined the isotopic fractionation and SP during production and reduction of N_2O , respectively.

2.1 Instrumentation

Bacterial production of N_2O was continuously measured by mid-infrared cavity ring-down spectroscopy using a prototype of the Picarro G5101-i analyzer (in the following named G5101i-CIC; Picarro, Santa Clara, California, USA). The measurements are non-destructive and are therefore suitable for incubation experiments. The CRDS instrument measures the $^{14}\text{N}^{14}\text{N}^{16}\text{O}$, $^{15}\text{N}^\alpha$ and $^{15}\text{N}^\beta$ absorption features of N_2O in the wavelength region between 2187.4 and 2188 cm^{-1} (Balslev-Clausen, 2011). The typical precision of the instrument over 10 min averaging is < 0.3 ppb for the N_2O mixing ratio and $< 0.4\%$ for each of the δ values of the isotopomers for concentrations in the range of 200–2000 ppb.

Measurements are made by a closed-loop gas flow through the G5101i-CIC with a microbial incubation glass chamber (Fig. 1). Circulation is provided by a leak-reduced diaphragm pump installed downstream from the analyzer. The pump (KNF N84.4 ANE) has been sealed using vacuum sealant (Celvaseal high-vacuum leak sealant, Myers Vacuum Repair Service, Inc., Kittanning, PA 16201, USA). A low leak rate is prerequisite for accurate measurements in a closed loop experiment. Upstream of the analyzer, a Nafion unit and an Ascarite trap is installed. The Nafion unit removes the bulk of H_2O vapor. Remaining water vapor is removed chemically by magnesium perchlorate ($\text{Mg}(\text{ClO}_4)_2$) in front and after

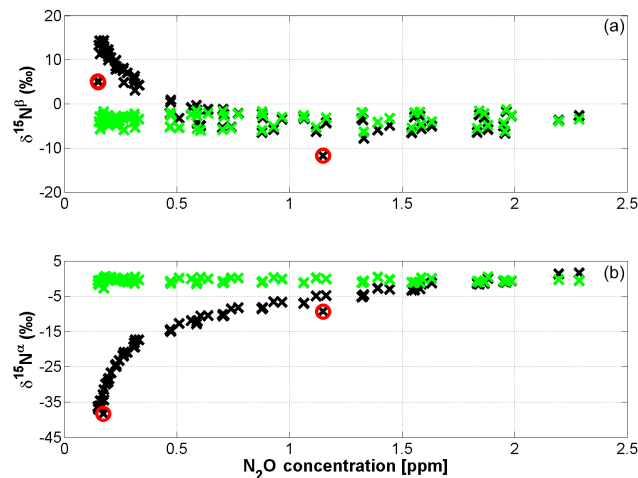


Figure 2. The concentration-dependent correction (CDC) for (a) $\delta^{15}\text{N}^\alpha$ and (b) $\delta^{15}\text{N}^\beta$. In both figures, the raw data are presented in black, the CDC data are plotted in green, and the outliers are marked with red circles.

the Ascarite (NaOH) section of the trap. Both gases are removed to exclude potential spectral interference with N_2O in the cavity of the analyzer. Underneath the glass chamber a magnetic stirrer is installed. The stirrer serves two purposes: (1) ensuring complete mixing of the bacterial solution and the added nutrient, i.e., potassium nitrate (KNO_3^-), and (2) facilitating gas exchange.

In addition to the measuring mode, the system can be flushed with N_2 (not shown in Fig. 1). The flushing mode is used to obtain an anaerobic starting point of the incubation experiment free of N_2O . The flushing procedure is fully automated to ensure reproducibility. The entire incubation setup is flushed with N_2 for 310 s at a high flow rate. The resulting overpressure in the incubator is released prior to switching back to the closed loop position.

2.2 Correction of CRDS concentration dependence

Isotopomer measurements made with the G5101i-CIC have a N_2O concentration dependence and need to be corrected. There is a $1/\text{concentration}$ dependence, caused by small offsets in the measurement of the $^{14}\text{N}^{15}\text{N}^{16}\text{O}$ and $^{15}\text{N}^{14}\text{N}^{16}\text{O}$ peaks. These offsets are caused by baseline ripple created by optical cavity etalons. An etalon is an optical effect in which a beam of light undergoes multiple reflections between two reflecting surfaces, and whose resulting optical transmission or reflection is periodic in wavelength. The ripples are not always constant in phase, which means that the ripples can shift spectrally, which can cause the offset to drift over time. Because baseline ripple effects become more dominant as N_2O concentration decreases, the offset is largest at low concentrations.

Figure 2 shows results from seven dilution experiments where we gradually mixed a pure N_2O gas with a N_2/O_2

mixture (20.1 % O₂ and 79.9 % N₂, purity 99.999 %). Measurements were performed in a 60 min stepwise (18 steps) sequence of both increasing and decreasing concentrations (Fig. 2).

We chose to fit the raw data with a cubic spline smoothing function (CSS function) (Brumback and Rice, 1998). The best fit of these CSS functions are found (using a smoothing parameter of $p = 0.999$) through regression analysis. Four outliers were identified to be outside the 2σ boundary and were removed from the data set (the red circles in Fig. 2). After these outliers were removed the best fit was found again ($p = 0.999$) and the concentration-dependent correction was applied as shown with the green profiles in Fig. 2. Over the course of the experiments, no further instrumental drift was observed.

2.3 Calibration gases

Our working standards are CIC-MPI-1 and CIC-MPI-2, prepared based on two standard gases provided by J. Kaiser at University of East Anglia (UEA), Norwich, United Kingdom. These standard gases, MPI-1 and MPI-2, are pure N₂O gases with different isotopic composition (Kaiser, 2002). In our laboratory, each of the standard gases was diluted with a N₂ / O₂ mixture (20.1 % O₂ and 79.9 % N₂, purity 99.999 %) resulting in the two new standard gases, CIC-MPI-1 and CIC-MPI-2. We had both CIC standard gases measured at four different laboratories to ensure consistent isotopic values (see Table 1). The gases were originally measured at University of East Anglia in Norwich, United Kingdom (UEA). After mixing the gases were measured 3 times using GC/IRMS measurements at Tokyo Institute of Technology in Japan. At the Institute for Marine and Atmospheric Research (IMAU), Utrecht, the Netherlands, the gases were measured 22 times using GC/IRMS. At the Centre for Ice and Climate in Copenhagen Denmark (CIC) the gases were measured continuously over 2 h. All measurements are reported relative to atmospheric N₂. The root-mean-square deviations (RMSDs) calculated from the three laboratories with respect to the original UAE data (Table 1) are similar to the RMSD calculated by Mohn et al. (2014). They present RMSD calculations based on gas measurements performed at 12 different laboratories using both IRMS and laser spectroscopy.

2.4 Pure bacterial cultures

The two bacterial cultures used in this study are both gram-negative bacteria with the capability to denitrify, i.e., reduce nitrate to gaseous nitrogen. Isolates were obtained from a sandy-loam-type agricultural soil (Roskilde Experimental Station) on 11 April 1983. One culture is a *Pseudomonas fluorescens*, bio-type D that reduces NO₃⁻ all the way to N₂. The second culture, *Pseudomonas chlororaphis*, is only capable of reducing NO₃⁻ to N₂O (Christensen and Bonde, 1985), which means that the nitrous oxide reductase is absent or at

least not active in this organism. The latter bacterium is contained in the American Type Culture Collection with accession number ATCC 43 928 (Christensen and Tiedje, 1988). The cultures were grown anoxic in 50 mL serum bottles with 1/10 tryptic soy broth (Difco) added 0.1 g KNO₃ L⁻¹. After 6 days of growth at room temperature (24 °C), *P. chlororaphis* had converted all N in NO₃⁻ into N₂O. The bacterial culture of *P. Fluorescens* was cultivated for 6 days at a slightly lower temperature (15 °C) to ensure that the cultures were in a comparable phase of potential activity when assayed for gas production/reduction activity. The 6-day-old cultures were used in the incubation experiment where it is conditional for the denitrifying process that organic carbon is available, that the concentration of oxygen is low, and that the concentration of NO₃⁻ is high (Wrage et al., 2001; Stuart Chapin III et al., 2002).

2.5 Bacterial incubation experiments

Bacterial solution (50 mL) of *P. chlororaphis* or *P. fluorescens* was placed in a Petri dish in the 1000 mL incubation chamber. Hereafter, the setup was flushed with pure N₂ (purity 99.9999 %) to ensure anaerobic conditions. To ensure no N₂O gas exchange prior to the experiment, the bacterial solution was left for 90 min under constant magnetic stirring. Then the incubation chamber was opened and the bacterial solution was fed with 2.5 and 15 mL of 0.45 mM KNO₃ for *P. chlororaphis* and *P. fluorescens*, respectively. The incubation experiment started by again flushing the setup with pure N₂ immediately after the addition of KNO₃.

A total of seven replicate incubations of the full denitrifying bacteria (*P. fluorescens*) and five replicate incubations of the denitrifying bacteria with no active nitrous oxide reductase (*P. chlororaphis*) were executed. All of the cultures were continuously measured from the moment KNO₃ was added to the bacterial incubations. We terminated experiments with *P. fluorescens* when the N₂O concentration was below 0.2 ppm. For *P. chlororaphis*, we defined the end of the experiment when the N₂O concentration had reached a constant level for 200 min.

Continuous measurements of the bacterial production of N₂O from *P. chlororaphis* were performed for approximately 500 min for each replica. All five replicas were measured within 1 week, starting at the same hour of the day and after equally long cultivation prior to the measurements. The bacterial evolution of N₂O production and reduction from *P. fluorescens* was continuously measured for about 1000 min. The seven replicas were measured during three 1-week measuring campaigns over the course of half a year, always with an equally long cultivation prior to measurements.

Our CIC-MPI standards contain N₂O in an O₂ / N₂ mixture while our incubation measurements were carried out in an N₂ atmosphere. This difference has a significant effect on the spectroscopy. We find a linear dependence similar to the one found by Erler et al. (2015). The presented data

Table 1. Measurements of standard gas CIC-MPI-1 and CIC-MPI-2, and of diluted MPI-1 and MPI-2 gases. Measurements were measured at the four respective institutes. The combined mean values (Cmean) and standard deviations are calculated from measurements performed at Tokyo Tech, IMAU, and CIC. The root-mean-square deviations (RMSDs) are calculated against the original University of East Anglia (UEA) data.

Std. gas	Institute	[N ₂ O] (ppb)	$\delta^{15}\text{N}^{\text{bulk}}$ (‰)	$\delta^{15}\text{N}^{\alpha}$ (‰)	$\delta^{15}\text{N}^{\beta}$ (‰)
MPI-1	UEA	–	1.00 ± 0.03	0.70 ± 0.90	1.30 ± 0.90
CIC-MPI-1					
	Tokyo Tech	1828.9 ± 4.9	1.34 ± 0.17	1.44 ± 0.09	1.24 ± 0.35
	IMAU	1919.3 ± 21.0	1.08 ± 0.10	2.31 ± 0.25	-0.15 ± 0.33
	CIC	1918.4 ± 2.3	2.62 ± 1.77	0.29 ± 2.44	4.95 ± 2.37
	Cmean	1909.8 ± 29.3	1.32 ± 0.82	1.94 ± 0.87	0.70 ± 1.42
	RMSD	–	0.96	1.05	2.27
MPI-2	UEA	–	-1.78 ± 0.03	12.40 ± 0.04	-15.90 ± 0.90
CIC-MPI-2					
	Tokyo Tech	1840.2 ± 32.1	-1.30 ± 0.06	12.79 ± 0.22	-15.41 ± 0.24
	IMAU	1865.9 ± 16.0	-1.68 ± 0.10	11.80 ± 0.37	-15.16 ± 0.46
	CIC	1827.2 ± 1.8	-0.15 ± 1.78	12.58 ± 2.51	-12.89 ± 2.35
	Cmean	1857.9 ± 19.2	-1.43 ± 0.82	12.01 ± 1.06	-14.87 ± 1.13
	RMSD	–	0.98	0.43	1.81

have been corrected for the effect, which is 15.27, 11.66, and 13.47‰ for $\delta^{15}\text{N}^{\alpha}$, $\delta^{15}\text{N}^{\beta}$, and $\delta^{15}\text{N}^{\text{bulk}}$, respectively (see Supplement). Given the leak rate of the system we estimate that the O₂ concentration has not increased by more than 0.002% over the course of the experiment. We therefore neglect the effect of a continuously increasing O₂ concentration and assume a constant O₂ concentration of 0%.

2.6 Determination of isotopic fractionation

Our incubation experiments are Rayleigh-type experiments. In the following, we determine the underlying isotope fractionation from the isotopic evolutions in the incubator under this assumption. Rayleigh fractionation describes the changing isotopic composition in the substrate and product of a unidirectional one-step reaction. Lord Rayleigh (1896) derived the equation for the fractionating isotope ratio of the substrate (Eq. 3) as follows:

$$\frac{R_s}{R_{s,0}} = f^{(\alpha_{p/s}-1)}, \quad (3)$$

where $R_{s,0}$ is the initial isotope ratio of the substrate, R_s is the isotope ratio of the substrate at time t , $\alpha_{p/s}$ is the fractionation factor of the product versus the substrate, and f is the unreacted fraction of substrate at time t . The corresponding equation for the isotopic ratio of the accumulated product $R_{p,\text{acc}}$ derives as given in Eq. (4).

$$R_{p,\text{acc}} = R_{s,0} \cdot \left(\frac{1 - f^{\alpha_{p/s}}}{1 - f} \right) \quad (4)$$

The isotopic fractionation is defined as $\epsilon = \alpha - 1$. We do not know the isotopic composition of KNO₃ used for our experiments. However, when all KNO₃ has reacted to N₂O, its isotopic composition is identical to the initial composition of KNO₃. The final isotopic values of N₂O for *P. chlororaphis* can therefore be used to estimate the initial composition of KNO₃. The initial isotopic composition of KNO₃ is calculated as the average of the end values for $\delta^{15}\text{N}^{\alpha}$ and $\delta^{15}\text{N}^{\beta}$ to $-3.08\text{‰} \pm 1.05$ (identical to the $\delta^{15}\text{N}^{\text{bulk}}$ value).

2.6.1 Fractionation associated with N₂O production

The fractionation associated with production of N₂O is the result of multiple reactions with various isotopic fractionations (Ostrom and Ostrom, 2011). Although, Ostrom and Ostrom (2011) argue that the fractionation observed during production of N₂O via reduction of NO₃⁻ can be treated as a net isotope effect with NO₃⁻ being the substrate and N₂O as the product. During production of N₂O, Eq. (4) is therefore used in calculation of the net fractionation factor and the net isotope effect of $\delta^{15}\text{N}^{\text{bulk}}$. For the two isotopomers Eq. (4) needs to be slightly modified (see Supplement). The SP isotopic fractionation is derived using the relationship $\epsilon_{\text{sp}} = \epsilon_{\alpha} - \epsilon_{\beta}$ as stated by Ostrom et al. (2007) and Well and Flessa (2009a).

2.6.2 Modifications to the Rayleigh model

To describe the evolution of the isotopomers during production of N₂O, the Rayleigh process is not directly applicable to the isotopomers as the two isotopomers both are direct prod-

ucts of the same denitrification process from the same batch of denitrifying bacteria and nitrate. The accumulated product for the two isotopomers can be determined (as presented in the Supplement). The calculations result in an isotopomer correction factor φ_α and φ_β for the two isotopomers, respectively.

$$\varphi_\alpha = \frac{\alpha_\alpha}{\alpha_{\text{bulk}}} \quad (5)$$

$$\varphi_\beta = \frac{\alpha_\beta}{\alpha_{\text{bulk}}} \quad (6)$$

The fractionation factor for the bulk is denoted α_{bulk} , while the fractionation factors for the two isotopomers are presented as α_α and α_β , respectively. The Rayleigh equation for the accumulated product of $\delta^{15}\text{N}^\alpha$ ($R_{\text{p,acc}}^\alpha$) is therefore as presented in Eq. (7), in which $R_{\text{p,acc}}^{\text{bulk}}$ is the accumulated product calculated for $\delta^{15}\text{N}^{\text{bulk}}$. A similar equation exists for $R_{\text{p,acc}}^\beta$, using $\delta^{15}\text{N}^\beta$ and φ_β :

$$R_{\text{p,acc}}^\alpha = R_{\text{p,acc}}^{\text{bulk}} \cdot \varphi_\alpha. \quad (7)$$

Equation (7) is valid for *P. chlororaphis*. For *P. fluorescens*, both an immediate reduction and an uptake reduction take place simultaneously with N_2O production due to the pre-experimental cultivation leading to activation of all enzymes in the bacterial solution. Part of the freshly produced N_2O is therefore immediately reduced to N_2 . This reduction is fractionating with fractionation factor α_α^R , α_β^R , and α_{bulk}^R , respectively, for each of the isotopomers and the bulk. The isotope imprint of the reduction on the remaining N_2O depends on the ratio between reduction rate and production rate, from here on referred to as the reduction correction parameter (γ). Assuming γ is constant (for one experiment see Fig. 3b) results in the following first-order approximation of the accumulated product including the isotope imprint of the reduction on the remaining N_2O ($R_{\text{p,r}}^\alpha$).

$$R_{\text{p,r}}^\alpha = \frac{R_{\text{p,acc}}^\alpha \cdot (1 - \alpha_\alpha^R \cdot \gamma)}{1 - \gamma} \quad (8)$$

Equation (8) is presented for $\delta^{15}\text{N}^\alpha$, though similar equations are used for both $\delta^{15}\text{N}^\beta$ and $\delta^{15}\text{N}^{\text{bulk}}$. For any calculated ratio the values are given in ‰ using the δ notation (Eq. 1).

2.6.3 Isotopic fractionation associated with N_2O reduction

The isotopic fractionation during reduction of N_2O to N_2 derives from Eq. (3). Equation (3) is valid for the bulk $^{15}\text{N}/^{14}\text{N}$ isotope ratios of N_2O ($\delta^{15}\text{N}^{\text{bulk}}$) and for both of the two isotopomer isotope ratios ($\delta^{15}\text{N}^\alpha$ and $\delta^{15}\text{N}^\beta$) (Mariotti et al., 1981; Menyailo and Hungate, 2006; Ostrom et al., 2007; Lewicka-Szczebak et al., 2014).

2.6.4 Fitting procedure

We determine the respective isotopic fractionation during production and reduction of N_2O for each of the bacterial strains assuming a Rayleigh-type process. The best fit (highest R^2) is found using an iterative approach between the measured data and the Rayleigh fractionation model for the accumulated product.

For *P. chlororaphis* (being a pure producer of N_2O) we use Eqs. (4) and (7) as the Rayleigh fractionation model for the $\delta^{15}\text{N}^{\text{bulk}}$ and the two isotopomers, respectively. We fit the Rayleigh fractionation model to the measured data. The highest R^2 values are iteratively found, using iterative determination of the fractionation factor during production of N_2O ($0 \leq \alpha \leq 1$). The limits of the unreacted fraction of the substrate (f) was set to $f_{\text{start}} = 1$ and $f_{\text{end}} = 0$.

Since N_2O is the product and the substrate for production and reduction, respectively, Eqs. (8) and (3) are applied for *P. fluorescens* to the corresponding process. We defined the section of net production as being from the start of the measurements until the net production (net emission) rate turns negative. From the calculations of the net production rates (see Fig. 3) we believe that N_2O production continues after the point of maximum concentration. However, at one point NO_3^- , NO_2^- and NO are fully consumed and *P. fluorescens* is forced to exclusively reduce N_2O . We defined the start of the section where *P. fluorescens* is only reducing N_2O to the point where both $\delta^{15}\text{N}^\alpha$ and $\delta^{15}\text{N}^\beta$ start decreasing. Between the end of the net production and the start of the exclusive reduction, no Rayleigh model can be fitted.

The fractionation factors resulting in the highest R^2 values are picked as the best fit fractionation factor for each specific evolution. In the calculations of the N_2O production from *P. fluorescens* the fractionation factor during N_2O reduction is required. We therefore first fit the Rayleigh fractionation model (Eq. 3) to the measured N_2O reduction data. The highest R^2 values are iteratively found, using (1) the extremes of the unreacted fraction of the substrate being $f_{\text{start}} = 1$ and $f_{\text{end}} = 0$ and (2) the fractionation factor during reduction of N_2O ($0 \leq \alpha \leq 2$). Secondly we fitted the Rayleigh fractionation model (Eq. 8) to the measured N_2O production data. The highest R^2 values are iteratively found by varying (1) the extremes of the unreacted fraction of the substrate (f_{start} and f_{end}) with $1 \leq f_{\text{start}} < f_{\text{end}} \leq 0$ as the boundary conditions, (2) the reduction correction parameter (γ) in the range $0 \leq \gamma \leq 1$, and (3) the fractionation factor during production of N_2O ($0 < \alpha < 1$), and using the fractionation factor during N_2O reduction (from calculations above).

Nitric oxide (NO) accumulation in the headspace can not be excluded from any of the presented N_2O production experiments. The effect of accumulation of NO in the headspace is assumed to be addressed by iterative determination of f_{end} and f_{start} (Tables 4 and 2 for *P. chlororaphis* and for *P. fluorescens*, respectively); hence no further adjustment is made.

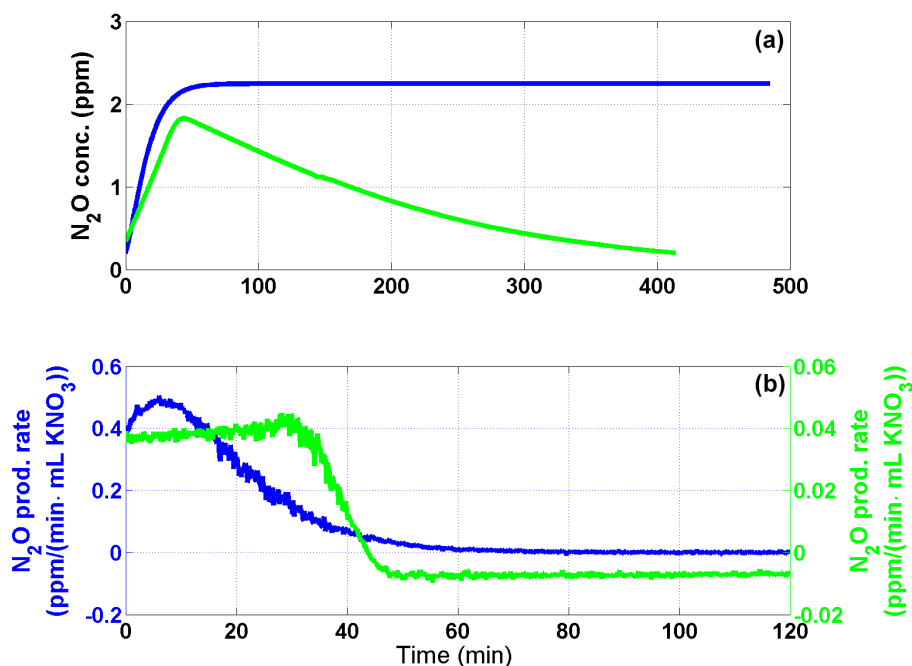


Figure 3. Continuous measurements of (a) N_2O concentrations and (b) the net N_2O production rate from experiments with *P. fluorescens* (green) and *P. chlororaphis* (blue), respectively. Only the first 120 min of the net N_2O production are shown. Note that the scaling of the two horizontal axes differs.

Table 2. Isotopic fractionation, reduction correction parameter (γ), extremes of the unreacted fraction parameter (f_{start} and f_{end}), and production rate (k_p) in $\text{ppm}(\text{min mL KNO}_3)^{-1}$ for the production of N_2O from *P. fluorescens*.

Replica no.	ϵ_α (‰)	ϵ_β (‰)	ϵ_{bulk} (‰)	ϵ_{SP} (‰)	γ	f_{start}	f_{end}	k_p
1	-55.50	-60.00	-57.75	4.50	0.00	0.38	0.000	0.035
2	-33.10	-32.50	-32.80	-0.60	0.52	0.94	0.000	0.078
3	-49.40	-54.40	-51.90	5.00	0.19	0.42	0.000	0.031
4	-59.80	-61.50	-60.65	1.70	0.00	0.68	0.000	0.016
5	-46.70	-58.50	-52.60	11.80	0.35	0.94	0.003	0.006
6	-56.40	-60.20	-58.30	3.80	0.04	0.69	0.007	0.005
7	-44.50	-58.40	-51.45	13.90	0.14	0.68	0.008	0.012
Mean	-49.34 ± 9.05	-55.07 ± 10.20	-52.21 ± 9.28	5.73 ± 5.26	0.18 ± 0.20	0.68 ± 0.22	0.003 ± 0.004	0.026 ± 0.026

3 Results

The evolution of N_2O concentration over time from the two bacterial strains shows two very distinctive patterns with both increasing and decreasing N_2O concentration characteristics for *P. fluorescens* and increasing N_2O concentration followed by stabilization for *P. chlororaphis* (Fig. 3a) as has previously been described by Christensen and Tiedje (1988). These distinctive characteristics are only vaguely seen in the respective dynamics of the SP for the two bacterial strains (Fig. 4a and b).

3.1 *Pseudomonas chlororaphis*

Paralleling the increase in N_2O concentration (Fig. 3a), we also find an increase in $\delta^{15}\text{N}^\alpha$, $\delta^{15}\text{N}^\beta$, and $\delta^{15}\text{N}^{\text{bulk}}$ over time

(Fig. 5a and b). The final product of *P. chlororaphis* is N_2O ; this is a unidirectional transfer of nitrogen from KNO_3 to N_2O and thereby a Rayleigh process although multiple fractionations are involved. Figure 5a and b show the best fit Rayleigh profile for $\delta^{15}\text{N}^\alpha$ and $\delta^{15}\text{N}^\beta$, respectively.

The modeled Rayleigh distillation profiles were found to match the production of N_2O from *P. chlororaphis* to a relatively high degree. The average coefficient of determination (R^2) between data and fitted Rayleigh curves are 72.15, 64.20, and 76.31 % for $\delta^{15}\text{N}^\alpha$, $\delta^{15}\text{N}^\beta$, and $\delta^{15}\text{N}^{\text{bulk}}$, respectively. The calculations of the isotopic fractionation for the fractionation of $\delta^{15}\text{N}^\alpha$ give a mean value of $-6.72\text{‰} \pm 1.54$ (Table 4). For $\delta^{15}\text{N}^\beta$ the mean isotopic fractionation was found to be $-3.28\text{‰} \pm 1.37$ (Table 4). These values lead to a mean SP isotopic fractionation value of $-3.42\text{‰} \pm 1.69$

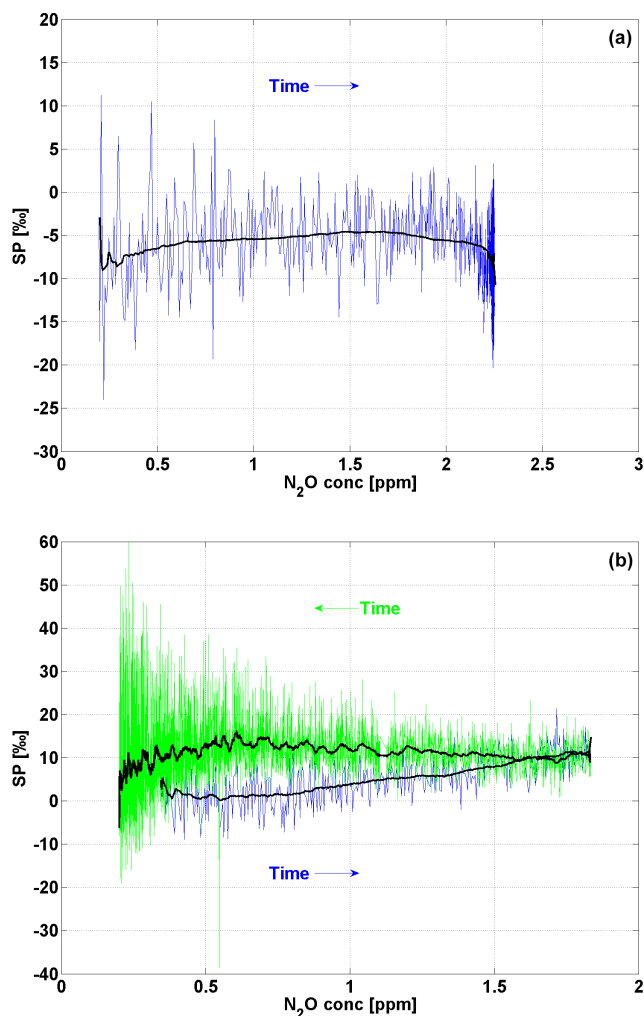


Figure 4. (a) SP as a function of N_2O concentration as produced by *P. chlororaphis*. High-resolution CRDS data (blue line) and 5 min running average (black line). The blue arrow indicates the direction of time during production of N_2O . (b) SP as a function of N_2O concentration produced by *P. fluorescens*. High-resolution CRDS data (blue and green line) and 5 min running average (black line). The blue arrow indicates the direction of time during production of N_2O whereas the green arrow indicates the direction of time during reduction of N_2O .

and a $\delta^{15}\text{N}^{\text{bulk}}$ isotopic fractionation of $-5.01\text{‰} \pm 1.20$ (Table 4).

3.2 Pseudomonas fluorescens

Continuous measurements of the evolution of N_2O produced and consumed by the denitrifying bacteria *P. fluorescens* are presented in Fig. 6a and b for $\delta^{15}\text{N}^{\alpha}$ and $\delta^{15}\text{N}^{\beta}$, respectively. The correlation coefficient of the fitted Rayleigh model for the production matches the continuously measured $\delta^{15}\text{N}^{\alpha}$ data by 94.44 % on average using the R^2 method for the seven replicates of *P. fluorescens* incubations. Equiva-

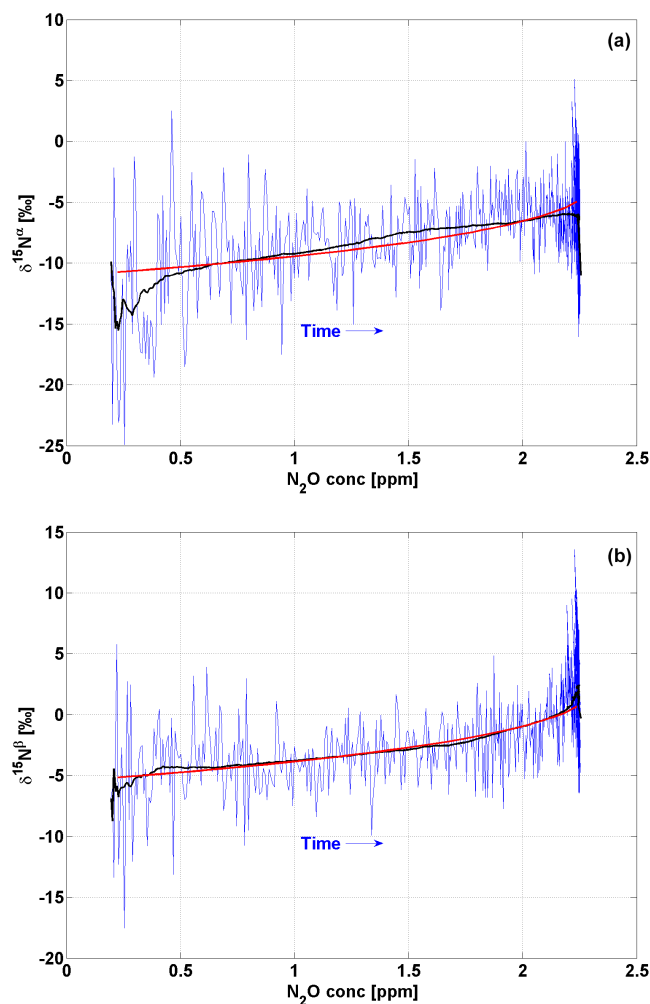


Figure 5. (a) $\delta^{15}\text{N}^{\alpha}$ as a function of N_2O concentration as produced by *P. chlororaphis* and the modeled Rayleigh-type distillation. High-resolution CRDS data (blue line) and 5 min running average (black line). The red curve is the modeled Rayleigh-type distillation curve for the production of N_2O . The blue arrow indicates the direction of time during production of N_2O . (b) $\delta^{15}\text{N}^{\beta}$ as a function of N_2O concentration as produced by *P. chlororaphis* and the modeled Rayleigh-type distillation. High-resolution CRDS data (blue line) and 5 min running average (black line). The red curve is the modeled Rayleigh-type distillation curve for the production of N_2O . The blue arrow indicates the direction of time during production of N_2O .

lent R^2 average for $\delta^{15}\text{N}^{\beta}$ are 94.13 %, whereas the average for $\delta^{15}\text{N}^{\text{bulk}}$ are found to be 96.86 %. The R^2 found for the reduction part is 91.92 % for $\delta^{15}\text{N}^{\alpha}$, 81.09 % for $\delta^{15}\text{N}^{\beta}$, and 92.42 % for $\delta^{15}\text{N}^{\text{bulk}}$ on average for the seven replicates. The fractionation during both the production and the reduction are therefore following the Rayleigh fractionation model to a large degree. The isotopic fractionation calculated using these models are therefore a good representation for the fractionation caused by the *P. fluorescens* bacteria on the

Table 3. Isotopic fractionation, extremes of the unreacted fraction parameter (f_{start} and f_{end}), and reduction rate (k_r) in k_p in ppm (min mL KNO_3)⁻¹ for the reduction of N_2O from *P. fluorescens*.

Replica no.	ϵ_α (‰)	ϵ_β (‰)	ϵ_{bulk} (‰)	ϵ_{SP} (‰)	f_{start}	f_{end}	k_r
1	9.70	7.10	8.30	2.60	1	0	-0.0027
2	3.10	4.10	3.40	-1.00	1	0	-0.0060
3	11.00	7.70	9.30	3.30	1	0	-0.0022
4	3.70	5.80	4.60	-2.10	1	0	-0.0027
5	18.20	11.70	14.80	6.50	1	0	-0.0014
6	17.10	12.30	14.50	4.80	1	0	-0.0019
7	9.30	6.50	6.50	2.80	1	0	-0.0009
Mean	10.30 ± 5.86	7.89 ± 3.04	8.77 ± 4.49	2.41 ± 3.04	1 ± 0	0 ± 0	-0.003 ± 1.7e ⁻³

Table 4. Isotopic fractionation, extremes of the unreacted fraction parameter (f_{start} and f_{end}), and production rate (k_p) in ppm (min mL KNO_3)⁻¹ for the production of N_2O from *P. chlororaphis*.

Replica no.	ϵ_α (‰)	ϵ_β (‰)	ϵ_{bulk} (‰)	ϵ_{SP} (‰)	f_{start}	f_{end}	k_p
1	-8.70	-3.10	-5.90	-5.60	1	0	0.237
2	-5.00	-1.10	-3.05	-3.90	1	0	0.250
3	-6.90	-3.30	-5.10	-3.60	1	0	0.215
4	-5.40	-4.40	-4.95	-0.90	1	0	0.182
5	-7.60	-4.50	-6.05	-3.10	1	0	0.126
Mean	-6.72 ± 1.54	-3.28 ± 1.37	-5.01 ± 1.20	-3.42 ± 1.69	1 ± 0	0 ± 0	0.201 ± 0.049

N_2O . The resulting isotopic fractionation is presented in Table 2 for the production part and in Table 3 for the reduction part together with the calculated isotopic fractionation for the SP. During production of N_2O , the mean isotopic fractionation for SP was found to be $\epsilon_{\text{SP}} = 5.73\text{‰} \pm 5.26$ while the $\epsilon_{\text{bulk}} = -52.21\text{‰} \pm 9.28$ for the $\delta^{15}\text{N}^{\text{bulk}}$; hence there is a difference of 9.15 and 47.20‰ for ϵ_{SP} and ϵ_{bulk} , respectively, to *P. chlororaphis*. During reduction of N_2O the mean isotopic fractionation for SP was found to be $\epsilon_{\text{SP}} = 2.41\text{‰} \pm 3.04$ and $\epsilon_{\text{bulk}} = 8.77\text{‰} \pm 4.49$ for $\delta^{15}\text{N}^{\text{bulk}}$.

4 Discussion

The two bacteria investigated are denitrifiers, in principle functionally similar but with *P. chlororaphis* lacking the ability to reduce N_2O to N_2 . Both denitrifiers were cultivated under anaerobic conditions leading to active nitric oxide reductase (both cultures) and nitrous oxide reductase (*P. fluorescens*). Fed the same amount of nitrate, we therefore expect the maximum N_2O concentration and the net N_2O production rate to be lower for *P. fluorescens* than for *P. chlororaphis*.

In Fig. 3, an example of the N_2O evolution by the two bacterial strains is plotted. The net N_2O production of *P. chlororaphis* is higher and a higher level in concentration is reached than by *P. fluorescens* even though *P. fluorescens* received 6 times more substrate than *P. chlororaphis*. These observations indicate that the nitrous oxide reductase consumes

N_2O from a very early stage of the N_2O turnover, likely because the cultures were grown under anaerobic conditions leaving both N_2O -producing and N_2O -consuming enzymes active from the beginning of the experiment.

N_2O produced by the two denitrifying bacteria differs primarily in the bulk isotopic fractionation whereas the SP isotopic fractionation averages at a more comparable level. We find that the average difference in isotopic fractionation between *P. chlororaphis* and *P. fluorescens* is 56.58 and 10‰ for ϵ_{bulk} and ϵ_{SP} , respectively (Fig. 7). That is, the isotopic fractionation is significantly higher for both isotopomers in *P. fluorescens* than in *P. chlororaphis*.

The observed difference in bulk isotopic fractionation during production of N_2O could originate from (1) a difference in the production rate, (2) a difference in the nitric oxide reductase enzymes, (3) a difference in nitrite reductase, or (4) fractionation caused by nitrous oxide reductase.

1. The production rates in our experiments (Tables 2 and 4) show a correlation between isotopic fractionation and production rate similar to the one observed by Mariotti et al. (1982). In our experiments the net production rate for *P. chlororaphis* is 10 times higher than for *P. fluorescens*, which would account for only approximately a 10‰ offset (cf. Mariotti et al., 1982). We therefore believe that a change in production rate does not account for the 56.58‰ difference in bulk isotopic fractionation alone.

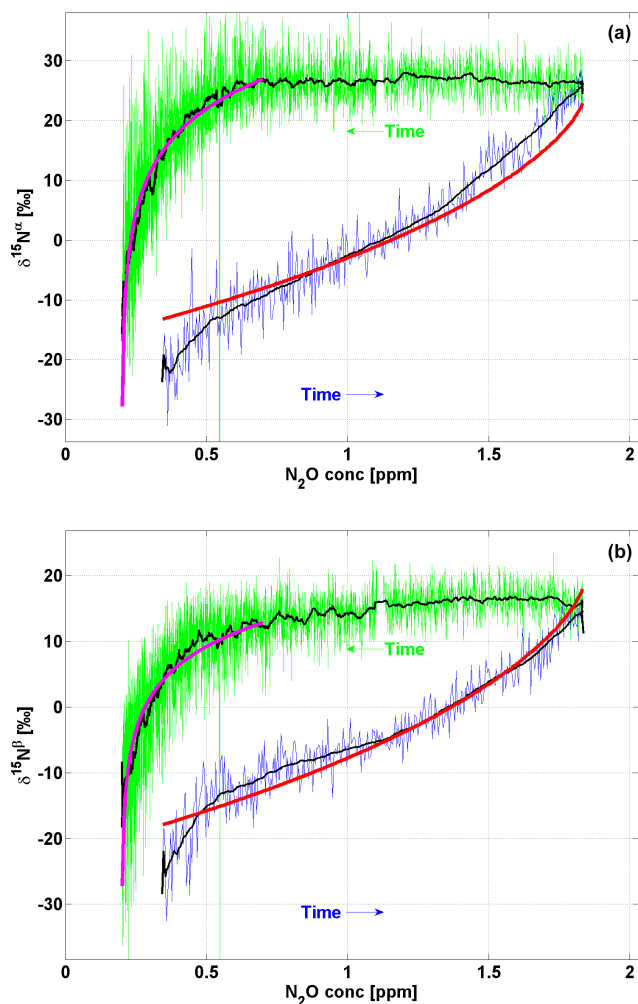


Figure 6. (a) $\delta^{15}\text{N}^{\alpha}$ as a function of N_2O concentration produced by *P. fluorescens* with the modeled Rayleigh-type distillation. High-resolution CRDS data (blue and green line) and 5 min running average (black line). The red and magenta curves are the modeled Rayleigh-type distillation curves for the production and reduction of N_2O , respectively. The blue arrow indicates the direction of time during production of N_2O whereas the green arrow indicates the direction of time during reduction of N_2O . (b) $\delta^{15}\text{N}^{\beta}$ as a function of N_2O concentration produced by *P. fluorescens* with the modeled Rayleigh-type distillation. High-resolution CRDS data (blue and green line) and 5 min running average (black line). The red and magenta curves are the modeled Rayleigh-type distillation curves for the production and reduction of N_2O , respectively. The blue arrow indicates the direction of time during production of N_2O whereas the green arrow indicates the direction of time during reduction of N_2O .

2. Nitric oxide reductase is the primary enzyme in a chain of catalytic reactions leading to the production of N_2O (Hino et al., 2010; Hendriks et al., 2000). The catalytic cycle involving production of N_2O from NO has yet to be completely understood with respect to the formation of the N–N double bond, the complexity of the struc-

tural information of nitric oxide reductase, the proton transfer pathway into nitric oxide reductase (Tosha and Shiro, 2013), and the very short lifetime of the intermediate states of the molecules (Collman et al., 2008). We hypothesized that the difference in the bulk observed during incubation of our two bacterial species was due to different nitric oxide reductases produced by the two species. To test this hypothesis, we compared the DNA sequences of the *norB* and *norC* genes coding for the large and small subunit of nitric oxide reductase, respectively, from three different strains of both *P. fluorescens* (strains NCIMB 11764, Genbank accession number CP010945; PA3G8, 742825335; and F113, CP003150) and *P. chlororaphis* (strains O6, 389686655; PA23, 749309655; and UFB2, 836582503), as well as from two closely related denitrifying species, *P. aeruginosa* and *P. stutzeri*. Our analysis revealed (i) a very high similarity of the two genes in *P. fluorescens* and *P. chlororaphis* and (ii) that the intra-species variability of the two genes was similar to the inter-species variation. This led us to reject our hypothesis and we conclude that differences in nitric oxide enzymes produced by the two species were not responsible for the observed differences in the bulk isotopic fractionation.

3. Nitrite reductase led to the first gaseous product during the denitrification pathway and it has been found to play an important role in isotope fractionation (Martin and Casciotti, 2016). The DNA sequences of the two bacterial strains used in our experiments revealed *P. chlororaphis* having a copper-containing nitrite reductase encoded by the gene *nirK*, while *P. fluorescens* has a heme-containing cytochrome cd1-type nitrite reductase encoded by the gene *nirS*. The two enzymes are structurally very different and show significantly different isotope fractionations on ϵ_{bulk} (Martin and Casciotti, 2016). Sutka and Ostrom (2006) conclude that a difference in the nitrite reductase does not have an effect on the SP during denitrification. This conclusion is based on measurements of two denitrifiers (*P. chlororaphis*, ATCC 43928; and *P. aureofaciens*, ATCC 13985) possessing cd1-type nitrite reductase and Cu-containing nitrite reductase, respectively. We conclude the same for the two denitrifying cultures presented in this work (*P. fluorescens* and *P. chlororaphis*) since the difference in isotopic fractionation between the two bacteria species is primarily in ϵ_{bulk} .
4. The experiments involving *P. fluorescens* are hypothesized to experience an increased fractionation during both production and reduction of N_2O as a result of simultaneous production and reduction of N_2O . After production of N_2O molecules, the light molecules degas quickly out of the liquid phase and away from the nitrous oxide reductase. The heavy N_2O molecules are

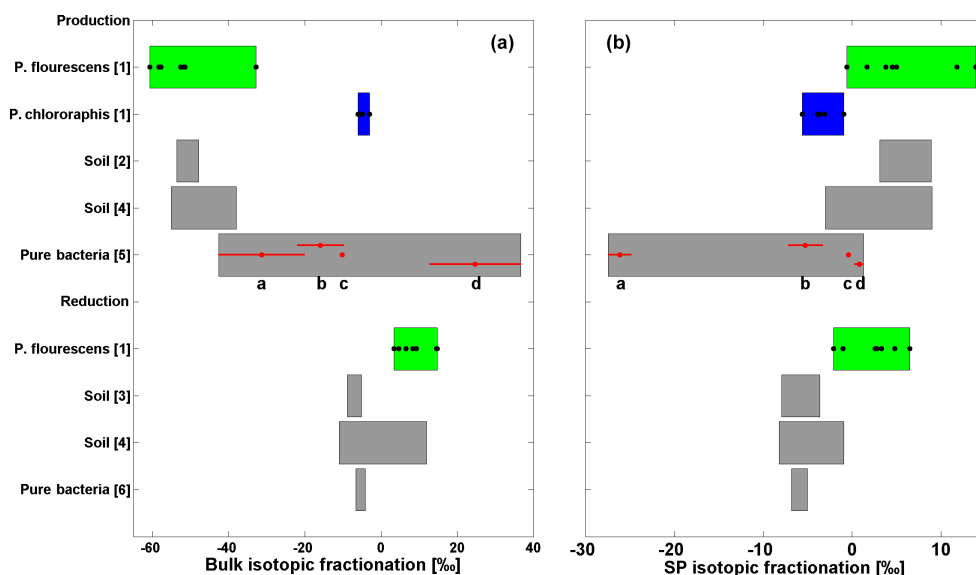


Figure 7. (a) Bulk and (b) SP isotopic fractionation calculated from the continuous measurements with *P. fluorescens* (green) and *P. chlororaphis* (blue), respectively. Both the production and reduction isotopic fractionations are shown and compared with previously presented results. [1] This study, [2] Well and Flessa (2009a), [3] Well and Flessa (2009b), [4] Lewicka-Szczebak et al. (2014, 2015), [5] (a) Thompson et al. (2004), (b) Toyoda et al. (2005), (c) Ostrom and Ostrom (2011), (d) Sutka and Ostrom (2006), and [6] Ostrom et al. (2007).

slower and react with the nitrous oxide reductase leading to a depletion of the heavy N_2O isotopes. As this is a diffusion-driven process, it is mass dependent and given the difference in bond energy required for breakage of the N–O bond a slight effect on SP is expected. This is also in line with the kinetic isotope effect theory which suggest a small offset towards higher ϵ_{α} and therefore higher ϵ_{SP} (Popp et al., 2002; Tilsner et al., 2003; Wrage et al., 2004; Well and Flessa, 2008).

We hypothesized that the difference in ϵ_{bulk} between the two bacteria originates from (1) a difference in production rates, (2) a difference in fractionation caused by different nitrite reductases, and (3) fractionation associated with nitrous oxide reductase in *P. fluorescens*. We also hypothesize that the slight difference in ϵ_{SP} originates predominantly from (4) fractionation associated with nitrous oxide reductase in *P. fluorescens*.

4.1 Comparison to previous studies

Numerous publications have presented experiments with both in situ measurements of denitrifying bacterial production and reduction of N_2O during incubation of bacterial cultures and soil samples. In Fig. 7, we present a comparison between the results from this study and the results from a selection of the previously published results. The general understanding is that denitrification results in $SP \leq 9\text{‰}$. Applying different incubation techniques on soils with different properties showed SP during production of N_2O between -3 and 9‰ and between -0.9 and -8.2‰ during

reduction (Well and Flessa, 2009a, b; Köster et al., 2013a; Lewicka-Szczebak et al., 2014, 2015). During production of N_2O in bacterial culture experiments (involving *P. chlororaphis*, ATCC 43928; *P. aureofaciens*, ATCC 13985; and *P. denitrificans*, ATCC 17741), Thompson et al. (2004), Toyoda et al. (2005), Sutka and Ostrom (2006), and Ostrom and Ostrom (2011) found ϵ_{SP} values of -27.4 and 1.3‰ and ϵ_{bulk} values of between -42.6 and 36.7‰ . The wide range of ϵ_{bulk} presented both in this study and by others confirms the difficulties in the use of ϵ_{bulk} in N_2O evolution analysis. Toyoda et al. (2005) present contrasting results for ϵ_{SP} of *P. fluorescens* (ATCC 13525) of 24.1‰ . The result may, however, not be comparable to ours as Toyoda et al. (2005) suspected an abiological reaction within the incubation flask to be responsible for N_2O production in the incubation experiment. Our results for ϵ_{SP} calculated during N_2O production from both *P. chlororaphis* and *P. fluorescens* are in the same range as what has been reported previously.

A number of studies have investigated N_2O reduction from denitrification in soils (e.g., Well and Flessa, 2009b; Köster et al., 2013a; Lewicka-Szczebak et al., 2014, 2015). The results are only partly in agreement with our findings for specific bacteria strains. While our results for ϵ_{bulk} are within the range of their findings, they find consistently negative ϵ_{SP} values while our results are generally positive. The only study on pure bacteria we know of is from Ostrom et al. (2007) for two bacteria strains different from ours, namely *P. stutzeri* and *P. denitrificans*. They found ϵ_{SP} values between -6.8 and -5‰ . At this point we have no explanation for the discrepancy but can find no artifact in our incubation setup.

5 Conclusions

We have presented successful continuous measurements of the denitrifying bacterial process using two different strains of bacteria: *P. fluorescens*, which is a full denitrifier, and *P. chlororaphis*, which is a denitrifier without nitrous oxide reductase activity. Assuming a Rayleigh-type fractionation, modified for isotopomers and simultaneous reduction, we have calculated the isotopic fractionation during production and reduction of N_2O . The isotopic fractionation for *P. chlororaphis* is in line with previous results for both SP and bulk. For *P. fluorescens*, we find similar SP isotopic fractionation values during N_2O production, while we find slightly increased SP isotopic fractionation values during N_2O reduction. The bulk isotopic fractionation calculated for N_2O reduction is in line with previously presented results though for production we find a bulk isotope depletion. We believe that, in our experiment, the bulk isotope depletion is due to a difference in production rates, in nitrite reductase, and in nitrous oxide reductase.

Data availability. The data have been uploaded to ERDA and are therefore available on the following permanent link: www.erda.dk/public/archives/YXJJaGl2ZS11M0Yyamk=/published-archive.html (Winther and Blunier, 2017).

The Supplement related to this article is available online at <https://doi.org/10.5194/bg-15-767-2018-supplement>.

Author contributions. MW and TB designed the experiments and MW carried out the measurements and analyzed data. SC prepared the bacteria prior to experiments. AP analyzed the bacterial DNA sequences. DBH and EC developed the G5101i-CIC analyzer. MW prepared the manuscript with contribution from all co-authors.

Competing interests. The authors declare that they have no conflict of interest.

Acknowledgements. We thank Jan Kaiser for isotope specific gas samples used for our reference gases, and Sakae Toyoda, Naohiro Yoshida, Carina van der Veen, and Thomas Röckmann for assistance in measurements of our reference gases. We want to thank the Center for Permafrost (CENPERM DNR100) and the Centre for Ice and Climate, funded by the Danish National Research Foundation for their support, and the Danish Agency for Science Technology and Innovation for the funding used in supporting this project. We want to thank Picarro Inc. and especially Eric Crosson and Nabil Saad for the collaboration and guidance in the development of the N_2O isotope analyzer prototype used in this project.

Edited by: Kees Jan van Groenigen

Reviewed by: two anonymous referees

References

- Balslev-Clausen, D. M.: Application of cavity ring down spectroscopy to isotopic bio- geo- & climate-sciences & the development of a mid-infrared CRDS analyzer for continuous measurements of N_2O isotopomers, PhD thesis, University of Copenhagen, 2011.
- Brenninkmeijer, C. A. M. and Röckmann, T.: Mass spectrometry of the intramolecular nitrogen isotope distribution of environmental nitrous oxide using fragment-ion analysis, *Rapid Commun. Mass Sp.*, 13, 2028–2033, [https://doi.org/10.1002/\(SICI\)1097-0231\(19991030\)13:20<2028::AID-RCM751>3.0.CO;2-J](https://doi.org/10.1002/(SICI)1097-0231(19991030)13:20<2028::AID-RCM751>3.0.CO;2-J), 1999.
- Brumback, B. A. and Rice, J. A.: Smoothing spline models for the analysis of nested and crossed samples of curves, *J. Am. Stat. Assoc.*, 93, 961–994, 1998.
- Christensen, S. and Bonde, G. J.: Seasonal variation in numbers and activity of denitrifier bacteria in soil. Taxonomy and physiological groups among isolates, *Danish Journal of Plant and Soil Science*, 89, 367–372, 1985.
- Christensen, S. and Tiedje, J. M.: Sub-parts-per-billion nitrate method: Use of an N_2O -producing denitrifier to convert NO_3^- or $^{15}NO_3^-$ to N_2O , *Applied and environmental microbiology*, 54, 1409–1413, 1988.
- Ciais, P., Sabine, C., Bala, B., Bopp, L., Brovkin, V., Canadell, J., Chhabra, A., DeFries, R., Galloway, J., Heimann, M., Jones, C., Le Quéré, C., Myneni, R., Piao, S., and Thornton, P.: 6: Carbon and Other Biogeochemical Cycles, in: Carbon and Other Biogeochemical Cycles, in: *Climate Change 2013: The Physical Science Basis. Contribution of Working Group I to the Fifth Assessment Report of the Intergovernmental Panel on Climate Change*, edited by: Stocker, T. F., Qin, D., Plattner, G.-K., Tignor, Cambridge University Press, Cambridge, United Kingdom and New York, NY, USA, 465–570, <https://doi.org/10.1017/CBO9781107415324.015>, 2013.
- Collman, J. P., Yang, Y., Dey, A., Decréau, R. A., Ghosh, S., Ohta, T., and Solomon, E. I.: A functional nitric oxide reductase model, *P. Natl. Acad. Sci. USA*, 105, 15660–15665, <https://doi.org/10.1073/pnas.0808606105>, 2008.
- Denk, T., Mohn, J., Decock, C., Lewicka-Szczebak, D., Harris, E., Butterbach-Bahl, K., Kiese, R., and Wolf, B.: The nitrogen cycle: A review of isotope effects and isotope modeling approaches, *Soil Biol. Biochem.*, 105, 121–137, <https://doi.org/10.1016/j.soilbio.2016.11.015>, 2017.
- Erler, D. V., Duncan, T. M., Murray, R., Maher, D. T., Santos, I. R., Gatland, J. R., Mangion, P., and Eyre, B. D.: Applying cavity ring-down spectroscopy for the measurement of dissolved nitrous oxide concentrations and bulk nitrogen isotopic composition in aquatic systems: Correcting for interferences and field application, *Limnol. Oceanogr.*, 13, 391–401, <https://doi.org/10.1002/lom3.10032>, 2015.
- Firestone, M. K. and Davidson, E. A.: Microbiological basis of NO and N_2O production and consumption in soil, *Life Sci. R.*, 47, 7–21, 1989.

- Forster, P., Ramaswamy, V., Artaxo, P., Bernsten, T., Betts, R., Fahey, D., Lean, J. H. J., Lowe, D., Myhre, G., Prinn, J. N. R., Raga, G., Schulz, M., and Dorland, R. V.: Climate Change 2007: The Physical Science Basis, Contribution of Working Group I to the Fourth Assessment Report of the Intergovernmental Panel on Climate Change, chap. Changes in Atmospheric Constituents and in Radiative Forcing, Cambridge University Press, Cambridge, United Kingdom and New York, NY, USA, 130–217, 2007.
- Hartmann, D., Klein Tank, A., Rusticucci, M., Alexander, L., Brönnimann, S., Charabi, Y., Dentener, F., Dlugokencky, E., Easterling, D., Kaplan, A., Soden, B., Thorne, P., Wild, M., and Zhai, P.: 2013: Observations: Atmosphere and Surface, in: Climate Change 2013: The Physical Science Basis. Contribution of Working Group I to the Fifth Assessment Report of the Intergovernmental Panel on Climate Change, Cambridge University Press, Cambridge, United Kingdom and New York, NY, USA, 2013.
- Heil, J., Wolf, B., Brüggemann, N., Emmenegger, L., Tuzson, B., Vereecken, H., and Mohn, J.: Site-specific ^{15}N isotopic signatures of abiotically produced N_2O , *Geochim. Cosmochim. Ac.*, 139, 72–82, <https://doi.org/10.1016/j.gca.2014.04.037>, 2014.
- Hendriks, J., Oubrie, A., Castresana, J., Urbani, A., Gemeinhardt, S., and Saraste, M.: Nitric oxide reductases in bacteria, *Biochim. Biophys. Acta*, 1459, 266–273, [https://doi.org/10.1016/S0005-2728\(00\)00161-4](https://doi.org/10.1016/S0005-2728(00)00161-4), 2000.
- Hino, T., Matsumoto, Y., Nagano, S., Sugimoto, H., Fukumori, Y., Murata, T., Iwata, S., and Shiro, Y.: Structural Basis of Biological N_2O Generation by Bacterial Nitric Oxide Reductase, *Science*, 330, 1666–1670, <https://doi.org/10.1126/science.1195591>, 2010.
- Kaiser, J.: Stable isotope investigations of atmospheric nitrous oxide, PhD thesis, Johannes Gutenberg-Universität Mainz, 2002.
- Kim, K. R. and Craig, H.: Nitrogen-15 and oxygen-18 characteristics of nitrous oxide: A global perspective, *Science*, 262, 1855–1857, 1993.
- Köster, J. R., Well, R., Dittert, K., Giesemann, A., Lewicka-Szczebak, D., Mühling, K. H., Herrmann, A., Lammel, J., and Senbayram, M.: Soil denitrification potential and its influence on N_2O reduction and N_2O isotopomer ratios, *Rapid Commun. Mass Sp.*, 27, 2363–2373, <https://doi.org/10.1002/rcm.6699>, 2013a.
- Köster, J. R., Well, R., Tuzson, B., Bol, R., Dittert, K., Giesemann, A., Emmenegger, L., Manninen, A., Cárdenas, L., and Mohn, J.: Novel laser spectroscopic technique for continuous analysis of N_2O isotopomers – Application and intercomparison with isotope ratio mass spectrometry, *Rapid Commun. Mass Sp.*, 27, 216–222, <https://doi.org/10.1002/rcm.6434>, 2013b.
- Lewicka-Szczebak, D., Well, R., Köster, J. R., Fuß, R., Senbayram, M., Dittert, K., and Flessa, H.: Experimental determinations of isotopic fractionation factors associated with N_2O production and reduction during denitrification in soils, *Geochim. Cosmochim. Ac.*, 134, 55–73, <https://doi.org/10.1016/j.gca.2014.03.010>, 2014.
- Lewicka-Szczebak, D., Well, R., Bol, R., Gregory, A., Matthews, G., Misselbrook, T., Whalley, W., and Cardenas, L.: Isotope fractionation factors controlling isotopocule signatures of soil-emitted N_2O produced by denitrification processes of various rates, *Rapid Commun. Mass Sp.*, 29, 269–282, <https://doi.org/10.1002/rcm.7102>, 2015.
- Lord Rayleigh, S. R.: Theoretical considerations respecting the separation of gases by diffusion and similar processes, *Philos. Mag. Ser.*, 5, 493–498, <https://doi.org/10.1080/14786449608620944>, 1896.
- Mariotti, A., Germon, J. C., Hubert, P., Kaiser, P., Letolle, R., Tardieux, A., and Tardieux, P.: Experimental determination of nitrogen kinetic isotope fractionation: some principles; illustration for the denitrification and nitrification processes, *Plant Soil*, 430, 413–430, 1981.
- Mariotti, A., Germon, J. C., and Leclerc, A.: Nitrogen isotope fractionation associated with the NO_2^- to N_2O step of denitrification in soils, *Can. J. Soil Sci.*, 62, 227–241, 1982.
- Martin, T. S. and Casciotti, K. L.: Nitrogen and oxygen isotopic fractionation during microbial nitrite reduction, *Limnol. Oceanogr.*, 61, 1134–1143, <https://doi.org/10.1002/lno.10278>, 2016.
- Menyailo, O. V. and Hungate, B. A.: Stable isotope discrimination during soil denitrification: Production and consumption of nitrous oxide, *Global Biogeochem. Cy.*, 20, GB3025, <https://doi.org/10.1029/2005GB002527>, 2006.
- Mohn, J., Guggenheim, C., Tuzson, B., Vollmer, M. K., Toyoda, S., Yoshida, N., and Emmenegger, L.: A liquid nitrogen-free preconcentration unit for measurements of ambient N_2O isotopomers by QCLAS, *Atmos. Meas. Tech.*, 3, 609–618, <https://doi.org/10.5194/amt-3-609-2010>, 2010.
- Mohn, J., Tuzson, B., Manninen, A., Yoshida, N., Toyoda, S., Brand, W. A., and Emmenegger, L.: Site selective real-time measurements of atmospheric N_2O isotopomers by laser spectroscopy, *Atmos. Meas. Tech.*, 5, 1601–1609, <https://doi.org/10.5194/amt-5-1601-2012>, 2012.
- Mohn, J., Wolf, B., Toyoda, S., Lin, C. T., Liang, M. C., Brüggemann, N., Wissel, H., Steiker, A. E., Dyckmans, J., Szweck, L., Ostrom, N. E., Casciotti, K. L., Forbes, M., Giesemann, A., Well, R., Doucett, R. R., Yarnes, C. T., Ridley, A. R., Kaiser, J., and Yoshida, N.: Interlaboratory assessment of nitrous oxide isotopomer analysis by isotope ratio mass spectrometry and laser spectroscopy: Current status and perspectives, *Rapid Commun. Mass Sp.*, 28, 1995–2007, <https://doi.org/10.1002/rcm.6982>, 2014.
- Mosier, A., Kroeze, C., and Nevison, C.: Closing the global N_2O budget: nitrous oxide emissions through the agricultural nitrogen cycle, *Nutr. Cycl. Agroecosys.*, 52, 225–248, 1998.
- Olivier, J. G. J., Bouwman, A. F., Van der Hoek, K. W., and Berdowski, J. J. M.: Global air emission inventories for anthropogenic sources of NO_x , NH_3 , and N_2O in 1990, *Environ. Pollut.*, 102, 135–148, 1998.
- Ostrom, N. E. and Ostrom, P. H.: The isotopomers of Nitrous oxide: Analytical considerations and application to resolution of microbial production pathways, in: *Handbook of Environmental Isotope Geochemistry*, edited by: Baskaran, M., Springer Berlin Heidelberg, Berlin, Heidelberg, 453–476, <https://doi.org/10.1007/978-3-642-10637-8>, 2011.
- Ostrom, N. E., Pitt, A., Sutka, R., Ostrom, P. H., Grandy, A. S., Huizinga, K. M., and Robertson, G. P.: Isotopologue effects during N_2O reduction in soils and in pure cultures of denitrifiers, *J. Geophys. Res.*, 112, G02005, <https://doi.org/10.1029/2006JG000287>, 2007.
- Park, S., Pérez, T., Boering, K. A., Trumbore, S. E., Gil, J., Marquina, S., and Tyler, S. C.: Can N_2O stable iso-

- topes and isotopomers be useful tools to characterize sources and microbial pathways of N₂O production and consumption in tropical soils?, *Global Biogeochem. Cy.*, 25, GB1001, <https://doi.org/10.1029/2009GB003615>, 2011.
- Pérez, T., Trumbore, S. C., Tyler, S. C., Davidson, E. A., Keller, M., and De Camargo, P. B.: Isotopic variability of N₂O emissions from tropical forest soils, *Global Biogeochem. Cy.*, 14, 525–535, 2000.
- Pérez, T., Trumbore, S. E., Tyler, S. C., Matson, P. A., Ortiz-Monasterio, I., Rahn, T., and Griffith, D. W. T.: Identifying the agricultural imprint on the global N₂O budget using stable isotopes, *J. Geophys. Res.*, 106, 9869–9878, <https://doi.org/10.1029/2000JD900809>, 2001.
- Popp, B. N., Westley, M. B., Toyoda, S., Miwa, T., Dore, J. E., Yoshida, N., Rust, T. M., Sansone, F. J., Russ, M. E., Ostrom, N. E., and Ostrom, P. H.: Nitrogen and oxygen isotopomeric constraints on the origins and sea-to-air flux of N₂O in the oligotrophic subtropical North Pacific gyre, *Global Biogeochem. Cy.*, 16, 12-1–12-10, <https://doi.org/10.1029/2001GB001806>, 2002.
- Schilt, A., Baumgartner, M., Schwander, J., Buiron, D., Capron, E., Chappellaz, J., Loulergue, L., Schüpbach, S., Spahni, R., Fischer, H., and Stocker, T. F.: Atmospheric nitrous oxide during the last 140,000 years, *Earth Planet. Sc. Lett.*, 300, 33–43, <https://doi.org/10.1016/j.epsl.2010.09.027>, 2010.
- Stuart Chapin III, F., Matson, P. A., and Mooney, H. A.: *Principles of terrestrial ecosystem ecology*, Springer-Verlag, New York, 2002.
- Sutka, R. L. and Ostrom, N. E.: Distinguishing nitrous oxide production from nitrification and denitrification on the basis of isotopomer abundances, *Appl. Environ. Microb.*, 72, 638–644, <https://doi.org/10.1128/AEM.72.1.638-644.2006>, 2006.
- Thompson, A. E., Park, S., Firestone, M., Amundson, R., and Boering, K.: Variable Nitrogen Isotope Effects Associated With N₂O Isotopologue Production: Towards an Understanding of Denitrification Mechanism, AGU Fall Meeting Abstracts, available at: <http://adsabs.harvard.edu/abs/2004AGUFM.B11C..03T>, 2004.
- Tilsner, J., Wrage, N., Lauf, J., and Gebauer, G.: Emission of gaseous nitrogen oxides from an extensively managed grassland in NE Bavaria, Germany. II. Stable isotope natural abundance of N₂O, *Biogeochemistry*, 63, 249–267, <https://doi.org/10.1023/A:1023316315550>, 2003.
- Tosha, T. and Shiro, Y.: Crystal structures of nitric oxide reductases provide key insights into functional conversion of respiratory enzymes, *IUBMB Life*, 65, 217–226, <https://doi.org/10.1002/iub.1135>, 2013.
- Toyoda, S., Yoshida, N., Miwa, T., Matsui, Y., Yamagishi, H., and Tsunogai, U.: Production mechanism and global budget of N₂O inferred from its isotopomers in the western North Pacific, *Geophys. Res. Lett.*, 29, 5–8, 2002.
- Toyoda, S., Mutobe, H., Yamagishi, H., Yoshida, N., and Tanji, Y.: Fractionation of N₂O isotopomers during production by denitrifier, *Soil Biol. Biochem.*, 37, 1535–1545, <https://doi.org/10.1016/j.soilbio.2005.01.009>, 2005.
- Waechter, H., Mohn, J., Tuzson, B., Emmenegger, L., and Sigrist, M. W.: Determination of N₂O isotopomers with quantum cascade laser based absorption spectroscopy, *Opt. Express*, 16, 9239–9244, <https://doi.org/10.1364/OE.16.00923>, 2008.
- Well, R. and Flessa, H.: Isotope fractionation factors of N₂O diffusion, *Rapid Commun. Mass Sp.*, 22, 2621–2628, <https://doi.org/10.1002/rcm>, 2008.
- Well, R. and Flessa, H.: Isotopologue signatures of N₂O produced by denitrification in soils, *J. Geophys. Res.*, 114, G02020, <https://doi.org/10.1029/2008JG000804>, 2009a.
- Well, R. and Flessa, H.: Isotopologue enrichment factors of N₂O reduction in soils, *Rapid Commun. Mass Sp.*, 23, 2996–3002, <https://doi.org/10.1002/rcm>, 2009b.
- Winther, M. and Blunier, T.: Data_Winther_et_al_2017.zip, available at: www.erda.dk/public/archives/YXJjaGl2ZS11M0Yyamk=/published-archive.html (last access: February 2018), Centre for Ice and Climate, Niels Bohr Institute, University of Copenhagen, 2017.
- Wrage, N., Velthof, G. L., Beusichem, M. L. V., and Oenema, O.: Role of nitrifier and denitrification in the production of nitrous oxide, *Soil Biol. Biochem.*, 33, 1723–1732, 2001.
- Wrage, N., Lauf, J., del Prado, A., Pinto, M., Pietrzak, S., Yamulki, S., Oenema, O., and Gebauer, G.: Distinguishing sources of N₂O in European grasslands by stable isotope analysis, *Rapid Commun. Mass Sp.*, 18, 1201–1207, <https://doi.org/10.1002/rcm.1461>, 2004.
- Yoshida, N. and Toyoda, S.: Constraining the atmospheric N₂O budget from intramolecular site preference in N₂O isotopomers, *Nature*, 405, 330–334, <https://doi.org/10.1038/35012558>, 2000.